

Poluprov. **1**, 1442 (1967) [Sov. Phys. Semiconductors **1**, 1203 (1967)].

<sup>38</sup>The temperature coefficient of  $E_G$  was assumed to be constant up to room temperature. The value 0.30 eV at 4.2 K is from C. R. Pidgeon and S. H. Groves, in *II-VI Semiconducting Compounds, 1967 International Conference*, edited by D. G. Thomas (W. A. Benjamin, New York, 1967), p. 1080. The value 0.15 eV at 300 K is from C. Veri , Phys. Status Solidi **17**, 889 (1966).

<sup>39</sup>W. Giriat, Phys. Letters **24A**, 515 (1967).

<sup>40</sup>W. Szymańska, Phys. Status Solidi **23**, 69 (1967).

<sup>41</sup>The value for A was chosen to yield intrinsic carrier concentrations at low temperature that agree with the experimental data of Galazka [Phys. Letters **32A**, 101 (1970)] and Ivanov-Omskii *et al.* (Ref. 42). Both Galazka and Schmit [J. Appl. Phys. **41**, 2876 (1970)] have used

sets of parameters slightly different from ours to calculate intrinsic carrier concentrations in HgTe. The parameters used here give results that agree closely with the data of Ivanov-Omskii *et al.* and are certainly adequate for the purposes of this paper; our calculation gives, for the intrinsic electron concentration,  $n_i = 1.46 \times 10^{15} \text{ cm}^{-3}$  at 4.2 K and  $n_i = 4.01 \times 10^{17} \text{ cm}^{-3}$  at 300 K. The results at all temperatures are sensitive to the value chosen for  $m_p$ ; the low-temperature results are particularly sensitive to A. Nevertheless, a fit to experimental data can still be obtained even if any one of the parameters is changed appreciably provided compensating changes are made in other parameters.

<sup>42</sup>V. I. Ivanov-Omskii, B. T. Kolomiets, V. K. Ogorodnikov, and K. P. Smekalova, Fiz. i Tekh. Poluprov. **4**, 264 (1970) [Sov. Phys. Semiconductors **4**, 214 (1970)].

## Optical Properties of Semiconducting VO<sub>2</sub> Films\*

Anibal Gavini<sup>†</sup> and Clarence C. Y. Kwan

*Superior Electronics Inc., 2255 Dandurand, Montreal, Quebec, Canada*

(Received 22 October 1971)

The reflectivity of a thick sputtered film of VO<sub>2</sub> has been measured in the energy range 0.5–11.0 eV at room temperature. The complex dielectric constant ( $\epsilon_1$ ,  $\epsilon_2$ ) and the complex index of refraction ( $n$ ,  $k$ ) have been obtained from the reflectivity measurements using the Kramers-Kronig relations. We have also measured the transverse electroabsorption spectrum of a thin sputtered film of VO<sub>2</sub> at liquid-nitrogen temperature. Comparison of the electroabsorption spectrum with theoretical predictions identifies the edge at 2.011 eV as corresponding to a direct transition at an  $M_0$  edge. In spite of the lack of a band-structure calculation for VO<sub>2</sub>, the singularities in  $\epsilon_2$  at 0.6, 1.04, 1.32, 1.82, 2.64, 3.6, 5.89, and 9.6 eV are assigned to specific interband transitions.

### I. INTRODUCTION

Transition-metal oxides which show a phase transition from a semiconducting to a metallic state have been the subject of considerable interest.<sup>1, 2</sup> Of all these materials VO<sub>2</sub> is the most interesting in terms of applications.<sup>3, 4</sup> The transition in VO<sub>2</sub>, which is a first-order semiconductor-to-metal transition, occurs at 68 °C. This transition is accompanied by a lattice distortion from a low-temperature monoclinic to a high-temperature tetragonal structure. The origin of this transition has been the subject of considerable controversy.<sup>1, 5–7</sup> The electrical and optical properties of VO<sub>2</sub> have been studied extensively.<sup>8–11</sup> However, in most cases the stoichiometry, chemical purity, and freedom from defects of the measured VO<sub>2</sub> have not been high, at least by the standards of semiconductor technology, and this fact has produced a very large dispersion in the published data.

The electronic contribution to the optical properties of VO<sub>2</sub> has been studied by Verleur *et al.*<sup>10</sup> and by Borisov *et al.*<sup>12</sup> The temperature and pres-

sure dependence of the energy gap has been measured by Ladd and Paul,<sup>13</sup> and photoemission measurements have been performed by Powell *et al.*<sup>14</sup> These measurements indicate that in the low-temperature phase VO<sub>2</sub> has an energy gap between 0.6 and 1.0 eV due to the crystal-field splitting of the uppermost partially filled vanadium 3*d* conduction band. Optical transitions at energies higher than 2.5 eV have been assigned to interband transitions between an oxygen 2*p* valence band and the lowest empty vanadium 3*d* conduction band.

Standard optical measurements, such as reflection and absorption, do not provide very high resolution for solids whose optical spectra show very large structureless backgrounds. Several modulation techniques have been developed in the last few years. By measuring the derivative of the optical spectrum with respect to some parameter, these techniques eliminate the background and enhance the structure to allow very precise determination of the energies of the transitions. These methods have proved to be useful in determining the energy of the interband transitions in semiconductors, in-

sulators, and even metals.<sup>15, 16</sup> We have applied the electroabsorption technique<sup>17</sup> to VO<sub>2</sub> films in the energy range 0.5–6.0 eV.

The analysis of the modulated spectrum requires a reasonably good knowledge of the optical constants of the unperturbed material. Values for the real and imaginary parts of the dielectric constant ( $\epsilon_1$  and  $\epsilon_2$ ) have been published previously.<sup>10, 12</sup> However, there are large differences between the values reported. Also in some cases the measurements have been performed on films which have not been completely characterized so as to make meaningful comparisons impossible. To obtain values for  $\epsilon_1$  and  $\epsilon_2$ , we performed measurements of the reflectivity of VO<sub>2</sub> films in the energy range 0.5–11.0 eV.

## II. EXPERIMENTAL TECHNIQUES

We shall describe in Sec. II A the techniques of sample preparation and in Secs. II B and II C the optical and electronic equipment used in these measurements.

### A. Sample Preparation

The VO<sub>2</sub> films used in this work were prepared by reactive sputtering of vanadium onto polished sapphire substrates in an argon-oxygen atmosphere<sup>18</sup> under carefully controlled conditions. Electron diffraction studies show that the films used in the measurements were composed of stoichiometric polycrystalline VO<sub>2</sub> with a grain size of approximately 600 Å. Films 8000 and 2100 Å

thick were used for reflection and electroabsorption measurements, respectively. The ratio of the conductivities above and below the metal-semiconductor transition temperature for both films was better than 1000:1. The electrical characteristics of this material are described in the conductivity ( $\sigma$ ) vs reciprocal temperature ( $T^{-1}$ ) plot for the 2100-Å film as shown in Fig. 1. The thin film was coated with two parallel nichrome-gold electrodes with a spacing of 0.5 mm. The sample was mounted with silicone grease on the cold finger of an optical cryostat cooled by liquid nitrogen.<sup>19</sup> The gap between the parallel electrodes was aligned with the 0.5×6.0-mm slit on the cold finger. When cooled to liquid-nitrogen temperature, the sample resistance measured across the electrodes was 10<sup>9</sup> Ω. A transverse electric field could then be applied to the sample without causing Joule heating.

### B. Optical Equipment

The optical equipment used in the reflection and electroabsorption measurements is very similar. The light sources used were a 650-W quartz-iodine tungsten-filament lamp in the visible and infrared region, a 150-W xenon arc in the ultraviolet region, and a hydrogen discharge in the vacuum-ultraviolet region. The dispersing element was a  $\frac{3}{4}$ -m Spex model No. 1702 monochromator with suitable gratings. The detectors used were an EMI 9635Q photomultiplier in the visible and ultraviolet, an RCA 7102 in the near infrared and a PbS photoconductive cell in the infrared. A spectral resolution of 10 Å was used in the ultraviolet, correspondingly smaller resolutions in the visible and infrared.

### C. Electronic Equipment

We used ac techniques throughout the measurements. The light was mechanically chopped at 89 Hz and synchronously detected with a Brookdeal system 40 lock-in amplifier. The reflectance measurements were performed point by point by taking the sample in and out of the beam. In the electroabsorption measurements two ac signals have to be detected simultaneously. These are (i) the signal at 89 Hz proportional to the product of the incident light on the sample times the transmissivity of the sample and (ii) the signal at the frequency of the modulating field, 200 Hz in our measurements, proportional to the product of the incident light times the electric-field-induced changes in the transmissivity. Both signals were detected using Brookdeal system 40 lock-in amplifiers, divided electronically and plotted on an  $x-t$  recorder as a function of the wavelength of the light. The ac modulating field was applied to the sample using a Kepco OPS2000 operational power supply, capable of delivering up to a 3000-V peak, driven by a square-wave generator. A dc bias was

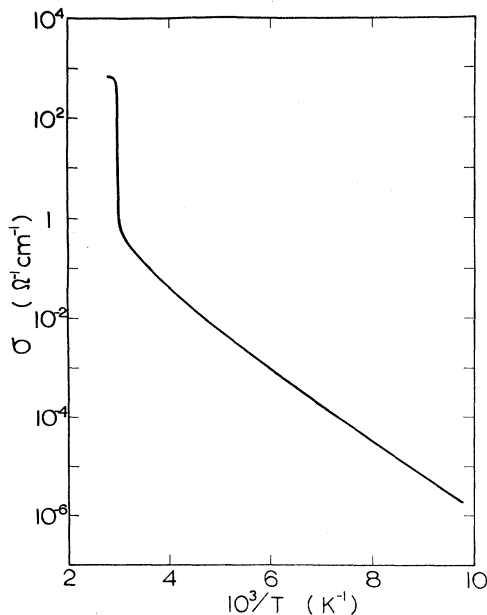


FIG. 1. Electrical conductivity of a 2100-Å-thick sputtered VO<sub>2</sub> film as a function of  $1/T$ .

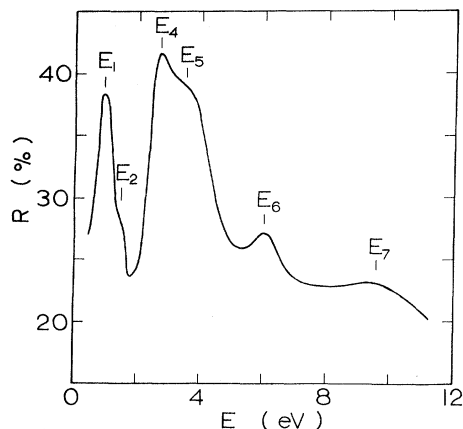


FIG. 2. Reflectivity spectrum of a VO<sub>2</sub> film at room temperature.

superimposed in order to modulate between zero and the maximum field.

### III. EXPERIMENTAL RESULTS

Figure 2 shows the room temperature reflectivity of an 8000 Å thick sputtered VO<sub>2</sub> film. Because of the thickness of the film no measurements were performed at energies lower than 0.5 eV. The general shape of the reflectivity spectrum is very similar to published results,<sup>10</sup> the main difference being the relative strength of the 1 eV peak to that of the 3 eV. In the reflectivity spectrum we can identify two main peaks, one at 1.04 eV labeled E<sub>1</sub> in Fig. 2, and a second one, which is really a doublet, labeled E<sub>4</sub>, E<sub>5</sub> at 2.64 and 3.56 eV, respectively. There is also some structure at higher energies; peaks E<sub>6</sub> and E<sub>7</sub> are at 6.0 and 9.6 eV, respectively. Figure 3 shows the transverse electroabsorption spectrum of a 2100-Å-thick sputtered VO<sub>2</sub> film. This measurement was performed at 80 K with an applied field ( $\vec{E}$ ) of  $5 \times 10^4$  V/cm. The samples had to be precooled before applying the field because of Joule heating at room temperature. The field dependence of the strength of the electroabsorption signal was measured for fields between  $10^4$  and  $5 \times 10^4$  V/cm. The strength of the signal was found to be proportional to the  $\frac{4}{3}$  power of the electric field. In spite of having performed measurements between 0.5 and 6.0 eV, we have only found the signal shown in Fig. 3. Our system has a sensitivity of one part in a million in its most sensitive region, i.e., from 2 to 3 eV. The sensitivity drops by at most a factor of five outside this range. No polarization effects were observed.

### IV. DATA ANALYSIS

The use of the Kramers-Kronig relations in the analysis of the reflectance data has been discussed in previous papers.<sup>20, 21</sup> These relations are

usually used in the following form:

$$\Theta(E_0) = \frac{E_0}{\pi} \int_0^{\infty} \frac{\ln R(E) - \ln R(E_0)}{E^2 - E_0^2} dE \quad (1)$$

to compute  $\Theta(E)$ , which is related to the optical constants by

$$\tan \Theta = -2k/(n^2 - k^2 - 1). \quad (2)$$

The Kramers-Kronig relations involve an integral over all energies; however, we have performed measurements only between 0.5 and 11.0 eV. We have extrapolated our results to  $E=0$  by using the values of the real part of the dielectric constant in the infrared in the absence of carriers.<sup>9</sup> To obtain the values of the reflectivity at energies higher than 11 eV, we have used the following asymptotic expression for the reflectivity for  $E > 11$  eV:

$$R(E) = qE^{-p}, \quad (3)$$

where  $q$  and  $p$  are parameters to be determined. We have determined  $p$  by making  $\Theta(E)$  go to zero at energies lower than the energy gap, a value of  $p = 2.2$  was found to give the best results. The parameter  $q$  was determined by making the reflectivity at high energies match the last measured value. The small value obtained for  $p$  is an indication that the reflectivity measurements have not been performed up to sufficiently high energies.

The results obtained for the real and imaginary parts of the dielectric constant are shown in Fig. 4. These results show a striking resemblance to those of Verleur *et al.*<sup>10</sup> for single crystals with light polarized parallel to the  $a_m$  axis. Apart from the peaks that have been identified in the reflectivity

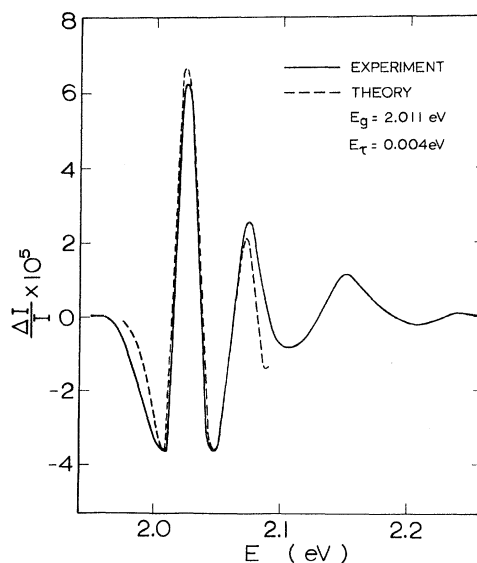


FIG. 3. Electroabsorption spectrum of a VO<sub>2</sub> film at 80 K,  $E = 5 \times 10^4$  V/cm.

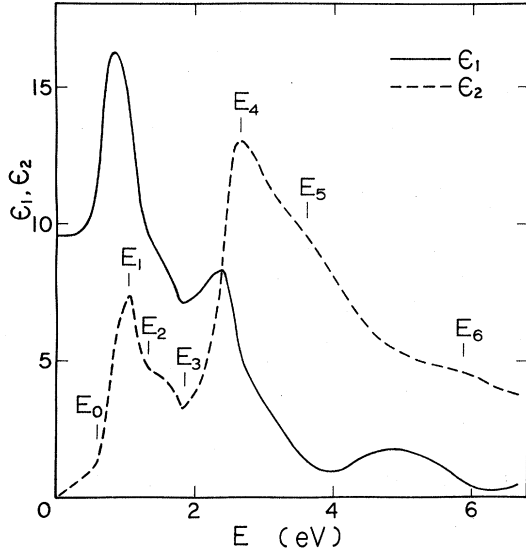


FIG. 4. Real ( $\epsilon_1$ ) and imaginary ( $\epsilon_2$ ) parts of the dielectric constant of VO<sub>2</sub> at room temperature.

two new thresholds  $E_0$  and  $E_3$  at 0.6 and 1.82 eV can be resolved. The  $E_0$  threshold corresponds to a definite change in the slope of  $R(E)$  and is not related to the extrapolation used for  $E < 0.5$  eV. The results for the index of refraction ( $n$ ) and the extinction coefficient ( $k$ ) are shown in Fig. 5, and those for the absorption coefficient ( $\alpha$ ) are shown in Fig. 6.

The effects of an electric field on the optical properties of semiconductors have been studied extensively. In particular, the electric-field-induced changes in the real and imaginary parts of the dielectric constant in the proximity of an interband edge have been the subject of several papers.<sup>22-24</sup>

The simplest method of calculating the effect of the electric field on allowed interband transitions around a Van Hove singularity of type  $M_0, M_1, M_2$ , or  $M_3$  involves the assumption of parabolic bands around the singularity and the use of the effective-mass approximation. The electric field  $\vec{E}$  is introduced as a perturbation to the unperturbed effective-mass Hamiltonian  $H_0$ :

$$H = H_0 - e\vec{E} \cdot \vec{r}. \quad (4)$$

To obtain the field-induced changes in the dielectric constant, we have to calculate only the interband matrix elements of the momentum operator, using as wave functions the eigenfunctions of  $H$ . It is possible to show that the changes in the real and imaginary parts of the dielectric constant can be expressed as functions of two universal electro-optic functions  $F$  and  $G$ .<sup>24</sup>

In the electroabsorption measurements we do not measure directly the changes in  $\epsilon_1$  or  $\epsilon_2$  but a com-

bination of them. In the range in which we have a nonzero signal and for the thickness of the sample used, the transmissivity of the sample can be written

$$I = I_0(1 - R)^2 e^{-\alpha d}, \quad (5)$$

where  $I_0$  is the incident light,  $R$  the reflectivity and  $d$  the thickness of the sample. The relative change in the transmissivity can be written

$$\frac{\Delta I}{I} = -\frac{2\Delta R}{1 - R} - d\Delta\alpha. \quad (6)$$

Taking into account the relationship of  $R$  and  $\alpha$  to  $\epsilon_1$  and  $\epsilon_2$ , it is possible to write (6) as

$$\Delta I/I = \alpha_1(\epsilon_1, \epsilon_2, E) \Delta\epsilon_1 + \alpha_2(\epsilon_1, \epsilon_2, E) \Delta\epsilon_2, \quad (7)$$

with

$$\alpha_1 = -\frac{1}{n^2 + k^2} \left( \frac{n^2 - 3k^2 - 1}{n^2 + k^2 + 2n + 1} - \frac{dEk}{\hbar c} \right), \quad (8)$$

$$\alpha_2 = -\frac{1}{n^2 + k^2} \left( \frac{(3n^2 - k^2 - 1)k}{(n^2 + k^2 + 2n + 1)n} + \frac{dEn}{\hbar c} \right).$$

The functions  $\alpha_1$  and  $\alpha_2$  can be computed using the values of  $\epsilon_1$  and  $\epsilon_2$  from Fig. 4. We have found that  $\alpha_2$  is practically independent of the energy and equal to  $-0.76$ ;  $\alpha_1$  however varies between 0.12 and 0.20 in the energy range 1.96–2.20 eV. These values together with the theoretical values obtained for  $\Delta\epsilon_1$  and  $\Delta\epsilon_2$ <sup>24</sup> were used to obtain the best fit to the experimental results. We found that broadening has to be introduced in order to obtain a good fit. Figure 3 shows the fit obtained for an  $M_0$  edge with a broadening parameter ( $E_\tau$ ) of 0.004 eV and an

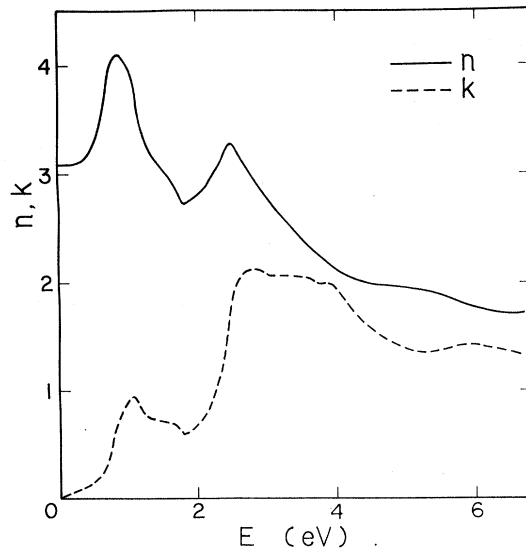


FIG. 5. Real ( $n$ ) and imaginary ( $k$ ) parts of the index of refraction of VO<sub>2</sub> at room temperature.

energy gap ( $E_g$ ) of 2.011 eV.

### V. DISCUSSION

Fine structure in the interband  $\epsilon_2$  spectrum is often obscured because  $\epsilon_2$  has been derived from an integral transform such as Eq. (1). In attempting to recognize structure, we should examine the experimental data, in our case  $R$ . However, in quoting edge energies to be compared with theory, we should refer to  $\epsilon_2$  as derived from the Kramers-Kronig relations.

We shall analyze the structure above and below 1.8 eV separately. (i)  $E < 1.8$  eV. In agreement with previous authors,<sup>10, 12</sup> we assign the  $E_0$ ,  $E_1$ , and  $E_2$  structure to transitions between the highest  $3d$  vanadium valence band and the lowest crystal-field-split  $3d$  conduction band. The large values of the absorption coefficient ( $10^5$  cm<sup>-1</sup> for  $E = 1$  eV) are an indication of strong hybridization of the  $3d$  vanadium bands with the  $2p$  oxygen bands. There is no definite threshold in the absorption coefficient;  $\alpha$  increases smoothly from  $10^3$  cm<sup>-1</sup> at 0.2 eV to  $10^5$  cm<sup>-1</sup> at 1 eV. This behavior can be explained as a combination of several effects: partially forbidden transitions, indirect transitions, and probably most important, sample imperfections (deviations from stoichiometry, impurities, etc.). Taking these facts into account, we assign the  $E_0$  threshold at 0.6 eV to the band gap and the  $E_1$  and  $E_2$  peaks to transitions between the same bands at other points in the Brillouin zone.

(ii)  $E > 1.8$  eV. The onset of the  $2p$ - $3d$  transitions has been described as lying somewhere be-

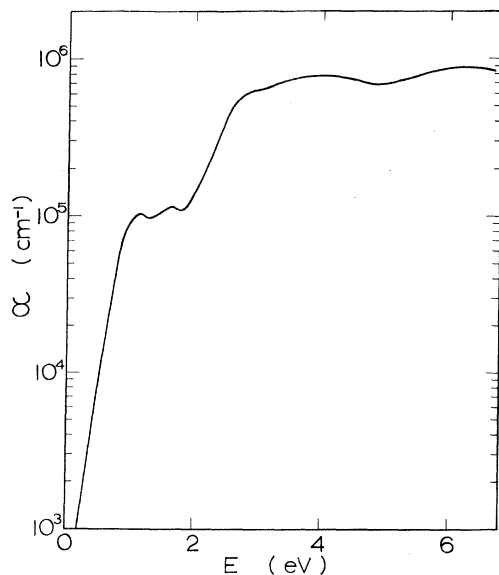


FIG. 6. Absorption coefficient ( $\alpha$ ) of  $\text{VO}_2$  at room temperature.

tween 2<sup>12</sup> and 2.5 eV.<sup>10, 12</sup> Based mainly in our electroabsorption measurements, we assign the  $E_3$  threshold to an  $M_0$ -type transition between the highest  $2p$  oxygen band and the lowest  $3d$  conduction band. The structure around 2.5 eV in the reflectivity spectrum of  $\text{VO}_2$  has usually been compared to that of  $\text{TiO}_2$  (rutile)<sup>10</sup>; however, we feel that it resembles more the results obtained for  $\text{BaTiO}_3$  at room temperature.<sup>25</sup> The crystallographic structure of tetragonal  $\text{VO}_2$ ,  $\text{TiO}_2$ , and  $\text{BaTiO}_3$  are quite similar in the sense that the titanium and vanadium atoms are situated in an oxygen environment of octahedral coordination. The reflectivity spectrum of  $\text{BaTiO}_3$  consists of an  $E_0$  threshold at 3.2 eV and a doublet  $A_1$ ,  $A_2$  at 3.91 and 4.85 eV, respectively. This structure is not only very similar to our results for  $\text{VO}_2$ , but the splitting of the doublet and the separation of the doublet from the  $E_0$  edge are virtually the same as that of the  $E_3$  threshold and  $E_4$ ,  $E_5$  doublet. The structure of the optical spectrum of  $\text{BaTiO}_3$  has been interpreted based on a band-structure calculation for  $\text{SrTiO}_3$ .<sup>26</sup> Following this interpretation, we assign the  $E_3$  threshold to a transition at  $\vec{K} = 0$ . The  $A_1$ ,  $A_2$  doublet has been assigned to transitions between the split  $p$  valence bands and the conduction band at  $\vec{K} = (1, 0, 0)$ .<sup>25</sup> In the case of  $\text{VO}_2$  the tetragonal field has already split the  $2p$  oxygen bands at  $\vec{K} = 0$  so is not possible to say at which point in the Brillouin zone these transitions occur.

It is very difficult to assign the high-energy structure to specific interband transitions. However, considering the width of the  $2p$  bands, the  $E_6$  peak probably corresponds to a transition between the  $2p$  bands and a higher-lying  $d$  band. The  $E_7$  peak can be assigned to a  $3d$ - $4p$  transition.

We shall now discuss the  $E_3$  threshold in somewhat more detail by considering the electroabsorption results. The position of the edge, 2.011 eV in the electroabsorption spectrum, agrees well with a value of 1.82 eV in  $\epsilon_2$  if we take into account the temperature dependence of the energy gap. As stated in Sec. IV, we have tried various possibilities to explain the measured line shape of the electroabsorption spectrum. The best fit obtained is shown in Fig. 3. The theoretical curve was calculated using Eq. (7) with the values of  $\Delta\epsilon_1$  and  $\Delta\epsilon_2$  obtained for an  $M_0$  edge.<sup>24</sup> In order to obtain a good fit of the relative strength of the peaks, broadening had to be introduced. We have used a broadening parameter ( $E_T$ ) of 0.004 eV, which is reasonable at 80 K. Another parameter that had to be introduced is the optical interband mass ( $m_0^*$ ). Taking into account the known value of the applied electric field,  $m_0^*$  was found to be  $0.12m_e$ . This value is lower than the reported values of  $m_c^* = 0.5m_e$ ,<sup>6</sup>  $0.8m_e$ ,<sup>12</sup> and  $4m_e$ <sup>9</sup> for the conduction electrons obtained from plasma-frequency mea-

surements and the estimate of from  $2m_e$  to  $7m_e$  obtained from transport measurements.<sup>8</sup> However, considering that the  $2p$  valence band is broader than the  $3d$  conduction band, the value obtained for  $m_0^*$  is very reasonable.

The field dependence of the strength of the electroabsorption signal was found to be

$$\Delta I/I \propto \bar{E}^{4/5}. \quad (9)$$

This value compares well with theoretical predictions for the intermediate field regime at which our measurements were performed and the broadening parameter used.<sup>24</sup>

The fact that no signal was observed for the  $E_0$ - $E_2$  structure can be explained by taking into account the relative weakness of the electroabsorption signal for forbidden transitions.<sup>16</sup> It is more difficult to explain why we have not seen any structure due to the  $E_4$ ,  $E_5$  doublet. One possibility could be phonon emission broadening of this structure. Since the  $E_4$ ,  $E_5$  transitions are most probably of  $M_1$  or  $M_2$  type, they are more sensitive to phonon

broadening at low temperatures than an  $M_0$ -type edge.

## VI. CONCLUSIONS

In conclusion we can say that we have unambiguously identified the threshold of the  $2p$ - $3d$  optical transitions in VO<sub>2</sub>. We have also obtained the first estimate of the optical interband mass for this transition. Based on a comparison with the optical spectra of BaTiO<sub>3</sub> we have been able to assign the observed structure in  $\epsilon_2$  to appropriate interband transitions. We have also obtained reliable data for the dielectric constant ( $\epsilon_1$ ,  $\epsilon_2$ ) and the index of refraction ( $n$ ,  $k$ ) for energies up to 11 eV.

## ACKNOWLEDGMENTS

We wish to thank Professor J. C. Woolley, University of Ottawa, for use of the optical cryostat; Dr. H. K. Eastwood and G. Karahoghossian for the material preparation; and Dr. R. Johannes for a critical reading of the manuscript.

\*Work supported in part by the National Research Council of Canada and the Defense Research Board of Canada through the industrial research program.

†Present address: Physics Department, Universidad de Buenos Aires, Buenos Aires, Argentina.

<sup>1</sup>D. Adler, in *Solid State Physics*, edited by F. Seitz, D. Turnbull, and H. Ehrenreich (Academic, New York, 1968), Vol. 21.

<sup>2</sup>Rev. Mod. Phys. **40**, 673-844 (1968).

<sup>3</sup>J. - I. Umeda, U. S. Patent 3,543,104 (Nov. 1970).

<sup>4</sup>W. Russell and C. H. Griffiths, in Proceedings of the International Electrical, Electronics Conference, Toronto, Canada, 1971 (unpublished).

<sup>5</sup>D. C. Mattis and W. D. Langer, Phys. Rev. Letters **25**, 376 (1970).

<sup>6</sup>J. B. Goodenough, J. Solid State Chem. (to be published).

<sup>7</sup>L. M. Falicov, McGill Summer School on Semiconductors, Montreal, Canada, 1971 (unpublished).

<sup>8</sup>C. N. Berglund and H. J. Guggenheim, Phys. Rev. **185**, 1022 (1969).

<sup>9</sup>A. S. Barker, Jr., H. W. Verleur, and H. J. Guggenheim, Phys. Rev. Letters **17**, 1286 (1966).

<sup>10</sup>H. W. Verleur, A. S. Barker, Jr., and C. N. Berglund, Phys. Rev. **172**, 788 (1968).

<sup>11</sup>W. Paul, Mat. Res. Bull. **5**, 691 (1970).

<sup>12</sup>B. S. Borisov, S. T. Koretskaya, V. G. Mokerov,

A. V. Rakov, and S. G. Solov'ev, Fiz. Tverd. Tela **12**, 2209 (1970) [Sov. Phys. Solid State **12**, 1763 (1971)].

<sup>13</sup>L. Ladd and W. Paul, Solid State Commun. **7**, 425 (1969).

<sup>14</sup>R. J. Powell, C. N. Berglund, and W. E. Spicer, Phys. Rev. **178**, 1410 (1969).

<sup>15</sup>B. O. Seraphin, in *Semiconductors and Semimetals*, edited by R. K. Willardson and A. C. Beer (Academic, New York, 1970), Vol. VI.

<sup>16</sup>M. Cardona, in *Solid State Physics*, edited by F. Seitz, D. Turnbull, and H. Ehrenreich (Academic, New York, 1969), Suppl. 11.

<sup>17</sup>Y. Yacoby, Phys. Rev. **142**, 445 (1966).

<sup>18</sup>C. C. Y. Kwan, C. H. Griffiths, and H. K. Eastwood (unpublished).

<sup>19</sup>C. C. Y. Kwan and J. C. Woolley, Phys. Status Solidi **44**, K93 (1971).

<sup>20</sup>F. C. Jahoda, Phys. Rev. **107**, 1261 (1957).

<sup>21</sup>M. Cardona and D. L. Greenaway, Phys. Rev. **133**, A1685 (1964).

<sup>22</sup>J. Callaway, Phys. Rev. **130**, 549 (1963).

<sup>23</sup>K. Tharmalingham, Phys. Rev. **130**, 2204 (1963).

<sup>24</sup>D. E. Aspnes, Phys. Rev. **147**, 554 (1966); **153**, 972 (1967).

<sup>25</sup>M. Cardona, Phys. Rev. **140**, A651 (1965).

<sup>26</sup>A. H. Kahn and A. J. Leyendeker, Phys. Rev. **135**, A1321 (1964).